Journal of Chromatography, 515 (1990) 125–148
Elsevier Science Publishers B.V., Amsterdam

CHROMSYMP. 1885

Fundamental study of hydroxyapatite high-performance liquid chromatography

III[a]. Direct experimental confirmation of the existence of two types of adsorbing surface on the hydroxyapatite crystal

TSUTOMU KAWASAKI*, MAKOTO NIIKURA and YURIKO KOBAYASHI
Chromatographic Research Laboratory, Koken Bioscience Institute, 3–5–18 Shimo-Ochiai, Shinjuku-Ku, Tokyo 161 (Japan)

ABSTRACT

By using several types of hydroxyapatite (HA) with different external shapes and surface structures, adsorption and the high-performance liquid chromatographic experiments for several proteins were carried out in parallel. Direct confirmation was obtained that two types of adsorbing surface, the **a** (or **b**) and the **c** crystal surface, generally appear on the HA particle. During the chromatographic process on the column, acidic proteins with isoelectric points lower than about 7 (and also nucleic acids including other nucleotides) are mainly adsorbed on the **a** (or **b**) surface, basic proteins with isoelectric points higher than about 7 are mainly adsorbed onto the **c** surface, and these occur independently of the external crystal shape of HA that is used. It is highly probable that the surface of a domain on the HA crystal on which the molecular adsorption takes place is smooth, and that the size of the domain under consideration is larger than the size of the proteins that have been applied, *i.e.*, larger than 100–200 Å, at least with respect to the HAs that have been examined. Multilayers of protein molecules may be formed on the HA surface when the molarity of the phosphate buffer in the mobile phase is much lower than the molarity that is needed for the migration of the molecules on the column.

INTRODUCTION

The hydroxyapatite (HA) crystal usually belongs in the space group $P6_3/m$, and the crystal unit cell is characterized by the primitive vectors **a**, **b** and **c** with $\mathbf{a} \wedge \mathbf{b} = 120°$, $\mathbf{a} \wedge \mathbf{c} = \mathbf{b} \wedge \mathbf{c} = 90°$, $|\mathbf{a}| = |\mathbf{b}| = 9.42$ Å and $|\mathbf{c}| = 6.88$ Å[3,4] (see also ref. 5). In a unit cell of the ideal stoichiometric crystal, ten calcium ions (Ca^{2+}), six phosphate ions (PO_4^{3-}) and two hydroxyl ions (OH^-) are arranged in the manner

[a] For Parts I and II, see refs. 1 and 2, respectively.

0021-9673/90/$03.50

represented in Fig. 1a. Therefore, the Ca/P molar ratio for the stoichiometric crystal is 1.67.

Fig. 2a–f show scanning electron micrographs of the surface structure of six types of HA particle to be packed in a column for high-performance liquid chromatography (HPLC). The Ca/P molar ratios for the crystals shown in Fig. 2a–f are 1.67, 1.67, 1.62, 1.57, 1.52–1.54 and 1.61–1.64, respectively. Therefore, the chemical compositions of the crystals in Fig. 2a and b are stoichiometric with respect to both calcium and phosphorus; the crystal structures of HA in Fig. 2c–f involve some defects.

The surface structure shown in Fig. 2a is quasi-ideal, and it can be identified that an HA particle is an aggregate of hexagonal rods each representing a crystallite or a micro-monocrystal. It can also be identified that the cross-sectional surface of a rod, hexagonal in shape, is an (001) surface or a **c** surface which is parallel to the (**a**, **b**) plane of the crystal unit cell; the six surfaces, rectangular in shape, occurring around the main axis of the rod are (100) or (010) surfaces, *i.e.*, **a** or **b** surfaces. These are parallel to the (**b**, **c**) or the (**a**, **c**) plane of the crystal unit cell (see Fig. 1a). (The **a** and the **b** surfaces are equivalent to each other; hereafter, except in certain instances, we simply use **a** surface for both **a** and **b** surfaces.) Thus, on a polycrystal of the type shown in Fig. 2a, only **a** and **c** surfaces appear; the total area of the **c** surfaces is much smaller than that of the **a** surfaces.

The HA shown in Fig. 2e is an aggregate of microcrystals with a needle-like shape. From the crystal habit, it is highly probable that the **c** axis is parallel to the main

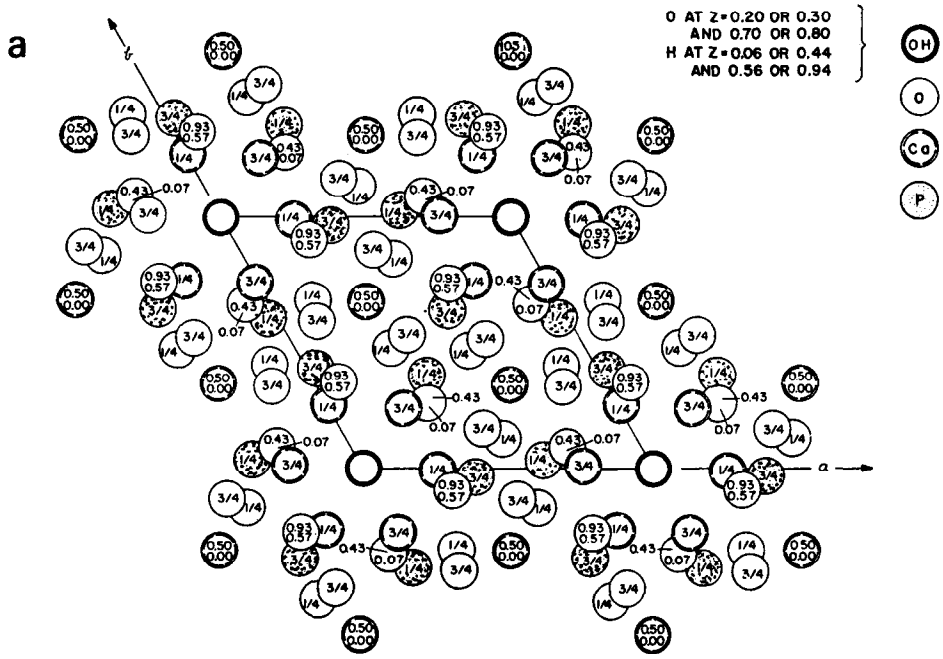

Fig. 1.

(*Continued on p. 127*)

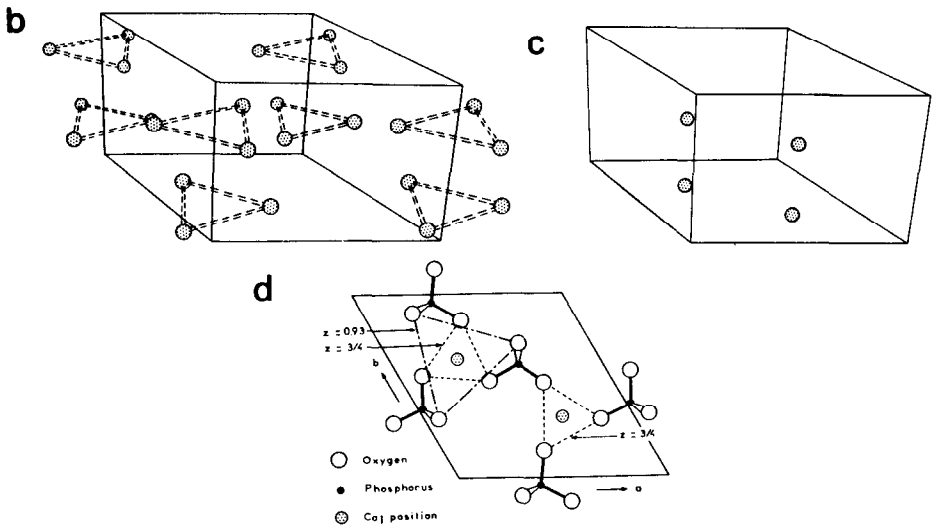

Fig. 1. (a) HA structure projected on the (**a**, **b**) plane along the **c** axis which is vertical to the plane of the paper. The parallelogram represents a crystal unit cell. The numerical values on the atoms represent z values, *i.e.*, coordinates along the **c** axis; z is equal to zero and unity at the lower and the upper margin of a unit cell, respectively. Calcium ions at $z = 0.00$ and 0.50 are called Ca_I ions, and those at $z = 1/4$ and $z = 3/4$ are called Ca_{II} ions. (Reproduced from ref. 3.) (b) Perspective view of Ca_{II} ions. The outline of the crystal unit cell is also drawn, where **a** is horizontally directed to the right in the plane of the paper, **b** is directed into the paper and **c** is vertical and upwards. It can be seen that there are a pair of triangular arrays of Ca_{II} ions centred on each edge (6_3 axis) of the unit cell, which lie on two mirror planes [parallel to the (**a**, **b**) plane] being at levels of $z = 1/4$ and $z = 3/4$, respectively. A pair of hydroxyl ions are also centred on each 6_3 axis, surrounded by the pair of triangular arrays of Ca_{II} ions, respectively. [Hydroxyl ions are not drawn; for the z values for the ions, see (a).] When the (**a** = **0**, **c** = **0**) or the (**b** = **0**, **c** = **0**) plane of the unit cell is on the crystal surface, one of the three Ca_{II} ions constituting a triangular array is outside the crystal; the two other Ca_{II} ions survive on the crystal surface, receding slightly behind the (**a** = **0**, **c** = **0**) or the (**b** = **0**, **c** = **0**) plane. It can be deduced that, when the HA crystal is suspended in an aqueous solution, the hydroxyl positions on the crystal surface, each inserted by two Ca_{II} ions, are void at least for an instant. (Reproduced from ref. 6. The above interpretation is given in ref. 7, however.) (c) Perspective view of Ca_I ions. It can be seen that there are two columns of Ca_I ions per unit cell along two three-fold rotatory symmetry axes, and that each column is constituted of two Ca_I ions occurring at $z = 0.00$ and 0.50 (nearly but not precisely at $z = 0$ and 1/2, respectively). (Reproduced from ref. 6.) (d) Deduced structure of the **c** surface of HA. It can be deduced that, when the HA crystal is suspended in an aqueous solution, two types of Ca_I position appearing on the **c** surface of HA are void at least for an instant. One of them is surrounded by six oxygen atoms (upper left) and the other is surrounded by three oxygen atoms (lower right). (Reproduced from ref. 8.)

axis of the "needle", and that most of the crystal surfaces appearing around the main axis of the "needle" are **a** surfaces.

With regard to the other crystals shown in Fig. 2b–d and f, however, it is difficult to identify the crystal surface on the basis of the electron micrograph only. (For the crystal surface of HA in Fig. 2f, see the third sub-section of the Discussion.)

A comparative study of the crystal structure of HA with that of octacalcium phosphate (OCP)[9,10] in combination with a study of the degradation mechanism of polyphosphates occurring on the crystal surface of HA[10,11] leads to the deduction that the **a** (or **b**) surface which just intersects the **b** (or **a**) axis of the crystal unit cell (see

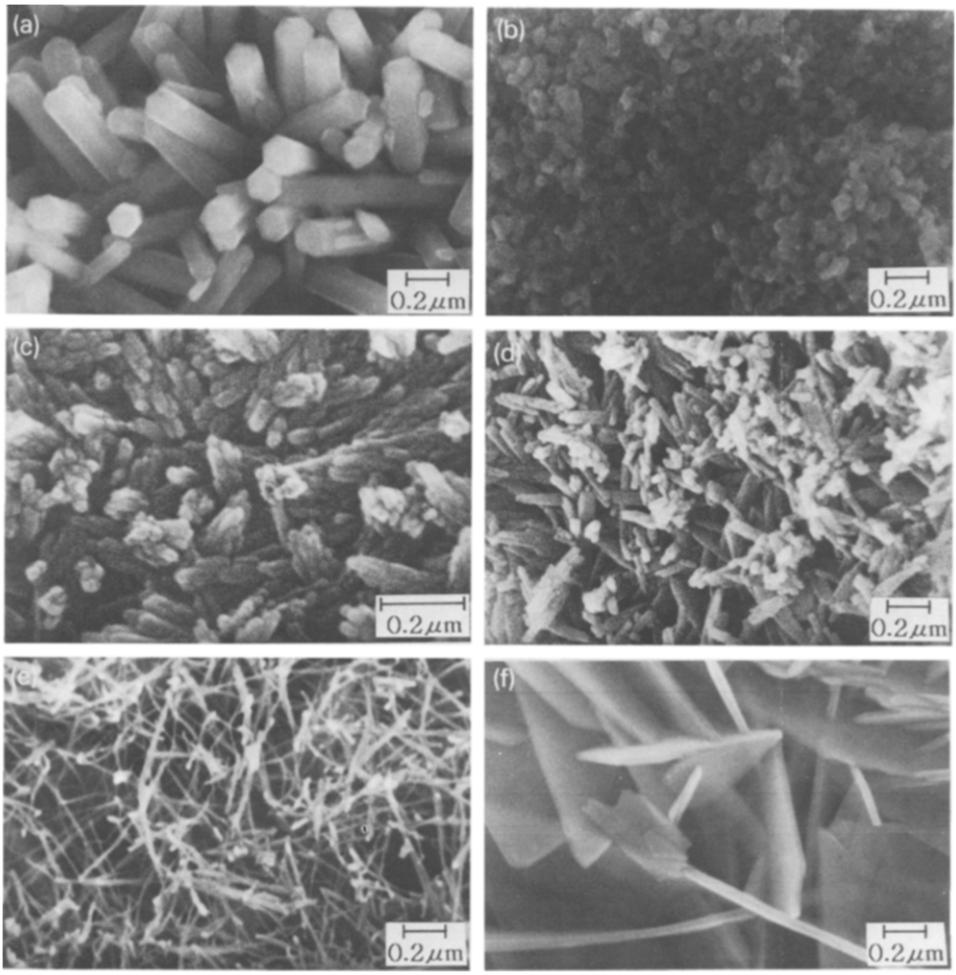

Fig. 2. Scanning electron micrographs of the surface structure of (a) coral HA with a Ca/P molar ratio of 1.67 (Mitsui Toatsu Chemicals, Tokyo, Japan), (b) spherical HA type S_1 with a Ca/P molar ratio of 1.67 (Koken), (c) HA type H with a Ca/P molar ratio of 1.62 (Koken), (d) HA type F with a Ca/P molar ratio of 1.57 (Koken), (e) potato-like HA with a Ca/P molar ratio of 1.52–1.54 (Central Glass) and (f) "rose des sables"-like HA with a Ca/P molar ratio of 1.61–1.64 (Central Glass). The entire image of HA type S_1 (b) is spherical with a diameter of about 5 μm. HA type H (c) is the Tiselius-type HA with a plate-like entire external shape. HA type F (d) has a square tile-like entire shape. The name "potato-like HA" (e) arises from the entire image of the crystal. "Rose des sables" (f) is a French word representing a gypsum "flower" produced naturally in the Sahara Desert.

Fig. 1a), in fact, appears on an HA crystal[7,10]. This means that positions at which hydroxyl ions should be present, provided that the positions are situated in the interior of the crystal, appear on the crystal surface, inserted by two Ca_{II} ions (see Fig. 1b; *cf.*, Fig. 1a). It can be deduced[7,10] that, when the HA crystal is suspended in an aqueous solution, the hydroxyl positions on the crystal surface, each inserted by two Ca_{II} ions, are void at least for an instant, and that the two Ca_{II} ions (with positive charges) constitute an adsorbing site (see Fig. 1b). It can further be deduced[7] that the site is

identical with the chromatographic C site, or the anion exchanger on which a competing phosphate ion from the phosphate buffer and a phosphate or a carboxyl group on the sample macromolecule are adsorbable (see previous papers[1,2]). (A free phosphate ion and a phosphate group on the macromolecule would be adsorbed directly on a hydroxyl position[7,10]. The possibility cannot be excluded, however, that a carboxyl group on the macromolecule is adsorbed on a position situated in the middle of two hydroxyl positions arranged in the **c** direction on the **a** surface of HA. This is because carbonic ions may be situated at corresponding positions in the interior of the crystal, excluding hydroxyl ions[6].) An image can finally be attained that, on the **a** (or **b**) surface of HA, adsorbing C sites are arranged in a rectangular manner with the interdistance in the **b** (or **a**) direction equal to $|\mathbf{b}|$ ($= |\mathbf{a}|$) = 9.42 Å and the interdistance in the **c** direction equal to $|\mathbf{c}|/2$ = 3.44 Å (*cf.*, Fig. 1b).

The mechanism of the adsorption of both free ions and adsorption groups of macromolecules on the crystal surface of HA resembles the first step of the epitaxial growth of the crystal (see Appendix II in ref. 8) where epitaxy consists in the growth of one crystal, in one or more particular orientations, on a substrate of another, with a near geometrical fit between the respective networks that are in contact[12]. In fact, if hydroxyl positions (C sites) on the **a** surface of HA are filled, under certain circumstances, with hydroxyl ions, then the crystal growth of HA would continue[7,10]. If hydroxyl positions are filled in an alternating manner with both phosphate ions and water molecules, then the epitaxial growth of OCP might begin on the **a** surface of HA[7,10].

It can be deduced that the **c** surface of HA is situated at the level of $z = 0.00$ or $z = 0.50$, as the exposure of another level of z on the crystal surface is only possible as compensation for the destruction of the chemical structure of crystal phosphate ions (see Appendix II in ref. 8). The levels, $z = 0.00$ and $z = 0.50$, equivalent to each other, are those where Ca_I ions should be present, provided the levels are situated in the interior of the HA crystal (see Fig. 1c; *cf.*, Fig. 1a). It can be deduced[8] that, when the HA crystal is suspended in an aqueous solution, the Ca_I positions on the crystal surface are void at least for an instant; two types of Ca_I position appear on the **c** surface of HA, one surrounded by six negatively charged oxygen atoms belonging to three crystal phosphates and the other surrounded by three negatively charged oxygen atoms belonging to three crystal phosphates (see Fig. 1d). It can be assumed[8] that the former Ca_I position is identical with the chromatographic P site, or the cation exchanger on which a competing sodium or potassium ion from the buffer and an ε-amino or a guanidinyl group on the protein molecule are adsorbable (see previous papers[1,2]); the latter Ca_I position may constitute a weak adsorbing site. An image can finally be attained that, on the **c** surface of HA, adsorbing P sites are arranged in a hexagonal manner with the minimum interdistance in both **a** and **b** directions equal to $|\mathbf{a}| = |\mathbf{b}|$ = 9.42 Å.

Of course, the possibility cannot be excluded that, owing to surface tension, the stereochemical structures of both **a** and **c** surfaces are distorted to a certain extent in comparison with the structure occurring in the interior of the crystal. It can be assumed, however, that the surface structure that has been deduced above represents the true structure to a good approximation.

In this work, by using several types of HA crystal with different external shapes and surface structures (Fig. 2a–f), adsorption and the HPLC experiments were carried

out in parallel; several proteins with different isoelectric points (pI) were used as probes. From these studies carried out with the aid of the study mentioned in the Introduction in Part II[2], a direct confirmation was obtained that, during the chromatographic process on the column, acidic proteins with p$I \lesssim 7$ (and also nucleic acids including other nucleotides) are mainly adsorbed on the **a** crystal surface, that basic proteins with p$I \gtrsim 7$ are mainly adsorbed on the **c** crystal surface and that these occur independently of the external crystal shape of HA that is used. This conclusion is consistent with the adsorption mechanism deduced from the structural study of HA with which the idea of the epitaxial crystal growth is connected (see above).

Further, profiles of the HPLC experiments obtained by using different types of HA were compared in detail. The results led to the deduction that the surface of a domain on the HA crystal on which the molecular adsorption takes place is smooth, and that the size of the domain under consideration is larger than the size of the proteins that have been applied, *i.e.*, larger than 100–200 Å. This means that the size of the crystallites that constitute the total crystal is larger than 100–200 Å, at least with respect to the HAs that have been examined.

From the analysis of overload chromatography, it can, in general, be deduced (see the last sub-section of Discussion) that a monolayer of sample molecules is formed on the crystal surface of HA when the development of the molecules is in progress on the column. On the basis of this study, the conclusion was drawn, however, that multi-layers of sample molecules may be formed on the HA surface when the molarity of the phosphate buffer in the mobile phase is much lower than that which is needed for the migration of the molecules on the column.

Concerning terminology, "acidic" and "basic" proteins are defined here as proteins that are eluted from the column with the second KP gradient and the first KCl gradient in the double gradient system, respectively (for the double gradient system, see Part II[2]; for KP, see the Experimental), whereas acidic and basic proteins mean proteins with pI values lower and higher than 7, respectively. "Acidic" and acidic proteins, and "basic" and basic proteins coincide with each other except in special cases (*cf.*, ref. 2; see also first sub-section of Discussion). (The abbreviations used in this paper are as follows: HA, hydroxyapatite; OCP, octacalcium phosphate; HPLC, high-performance liquid chromatography; ϕ, column I.D.; KP, potassium phosphate buffer, pH $\approx$ 6.8; P, pressure drop; T, temperature; pI, isoelectric point; BSA, bovine serum albumin; RNase A, ribonuclease A; IgG, immunoglobulin G; and m.h.h., mean height of the histogram.)

EXPERIMENTAL

In SUS316 stainless-steel columns of I.D. $\phi = 6$ mm, the following HA particles were packed: (a) coral HA constructed with hexagonal rods (Ca/P molar ratio = 1.67) (Mitsui Toatsu Chemicals, Tokyo, Japan) (see Fig. 2a), (b) spherical HA with a diameter of about 5 μm, called HA type S_1 (Ca/P molar ratio = 1.67) (Koken, Tokyo, Japan) (see Fig. 2b), (c) Tiselius-type plate-like HA, called HA type H (Ca/P molar ratio = 1.62) (Koken) (see Fig. 2c), (d) square tile-shaped HA, called HA type F (Ca/P molar ratio = 1.57) (Koken) (see Fig. 2d), (e) potato-like HA constructed with "needles" (Ca/P molar ratio = 1.52–1.54) (Central Glass, Tokyo, Japan) (see Fig. 2e) and (f) "rose des sables"-like HA constructed with lamellae (Ca/P molar ratio =

1.61–1.64) (Central Glass) (see Fig. 2f). For the adsorption experiments with proteins, a column of length 3 cm was used. For the HPLC experiments, columns with lengths of 3, 10 and 30 cm were prepared, and the 3-cm column was used as either a precolumn or a main column.

The adsorption experiments with proteins were carried out as follows. By using the same method as for HPLC, the sample molecules dissolved in 1 m*M* potassium phosphate buffer, pH $\approx$ 6.8 (composed of equimolar K_2HPO_4 and KH_2PO_4; called KP buffer), was injected, with a flow-rate of 0.5 ml/min, into a 3-cm column; this was followed by rinsing for 5–10 min with 1 m*M* KP buffer. In some experiments with cytochrome *c*, however, 1 m*M* KP was replaced with 50 m*M* KP. The column contents (*i.e.*, HA particles) were extruded from the inlet of the column by pushing them from the outlet with a rod. The cylindrical mass of the HA particles extruded from the column was cut into slices with a thickness of 2 mm; each was then suspended in 5 ml of 0.5 *M* KP with agitation in order to dissolve the sample molecules that had been captured on the HA surfaces into solution. The suspension was centrifuged and the absorbance of the supernatant at 230, 280 and/or 415 nm was measured in order to determine the total amount of the sample molecules that had been present in the slice.

The method used in the HPLC experiments, except preliminary double gradient HPLC, is decribed in the first sub-section of Experimental and Results in the preceding paper[2]. The sample elution was monitored by measuring the ultraviolet absorption at either 230 or 280 nm, however. With regard to the preliminary double gradient HPLC carried out by using 3 + 10 (= 13) cm column systems packed with coral HA, HA type S_1, HA type H, HA type F, potato-like HA and "rose des sables"-like HA, a KCl gradient, with $g'_{(KCl)}$ (ϕ = 1 cm) = 3.75 m*M*/ml, was first applied after isocratic elution with 10 m*M* KP; 10 m*M* KP was always present while the KCl gradient continued. The carrier solvent was again replaced with pure 10 m*M* KP, and the KP gradient, with $g'_{(P;KP)}$ (ϕ = 1 cm) = 2.5 m*M*/ml, was finally applied; 10 m*M* KP was replaced with 1 m*M* KP with both pepsinogen and ovalbumin, however. The final molarities of the KCl gradient in the double gradient system were nearly constant in the vicinity of 0.5 *M*. [For the symbols $g'_{(KCl)}$ (ϕ = 1 cm) and $g'_{(P;KP)}$ (ϕ = 1 cm), see the third sub-section of Experimental and Results in Part II[2].]

The sample molecules applied in the experiments were albumin (from bovine serum; Nutritional Biochemicals), lysozyme (from chicken egg white; P-L Biochemicals), pepsinogen (from hog stomach mucosa; Tokyo Kasei Kogyo), ovalbumin (from chicken egg white; Sigma, St. Louis, MO, U.S.A.), myoglobin (from sperm whale skeltal muscle; Sigma), trypsinogen (from bovine pancreas; Sigma), ribonuclease A (from bovine pancreas; Sigma), cytochrome *c* (from horse heart; Sigma), β-lactoglobulin A (from bovine milk; Sigma) and fractions I, II and III of immunoglobulin G (human; Japanese Red Cross Plasma Fractionation Centre, Tokyo, Japan) (for the three fractions of immunoglobulin G, see ref. 2, Appendix II).

RESULTS

Adsorption experiments on proteins: initial molecular band formed in the vicinity of the column inlet

The histograms in Fig. 3 show typical examples of the initial adsorptions of BSA (with an acidic p*I* of 4.7) and lysozyme (with a basic p*I* of 10.5–11.0) obtained in the

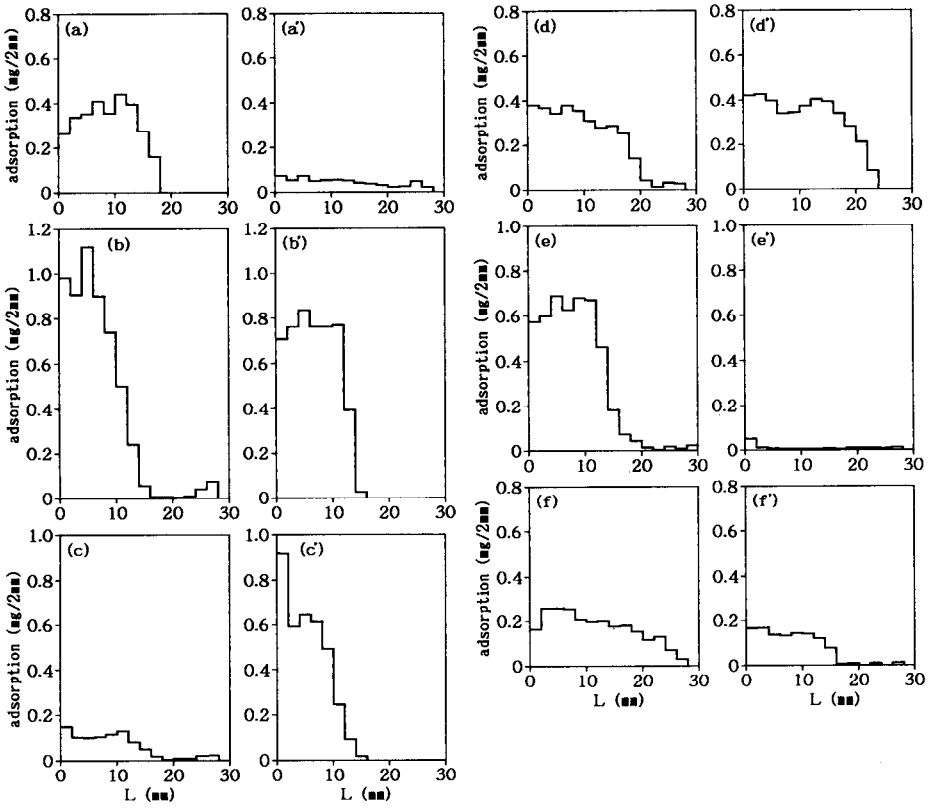

Fig. 3. Amounts of BSA (a–f) and lysozyme (a′–f′) adsorbed per 2 mm slice of the column contents (with ϕ = 6 mm) in the presence of 1 m*M* KP as functions of the distance, *L*, from the column inlet. The types of crystal packed in the column are coral HA for (a) and (a′), HA type S_1 for (b) and (b′), HA type H for (c) and (c′), HA type F for (d) and (d′), potato-like HA for (e) and (e′) and "rose des sables"-like HA for (f) and (f′).

presence of 1 m*M* KP. These are drawn as functions of the distance, *L*, from the inlet of the columns packed with six different types of HA; the amount of molecules involved in a 2-mm slice of the column contents is represented by a portion of the histogram with a width of 2 mm (see Experimental). Hence, the histograms in Fig. 3a–f represent those for BSA obtained by using columns packed with coral HA (Fig. 2a), HA type S_1 (Fig. 2b), HA type H (Fig. 2c), HA type F (Fig. 2d), potato-like HA (Fig. 2e) and "rose des sables"-like HA (Fig. 2f), respectively. The histograms in Fig. 3a′–f′ are for lysozyme corresponding to those in Fig. 3a–f, respectively. It can be seen in Fig. 3 that, with both coral HA (constructed with hexagonal rods; Fig. 2a) and potato-like HA (constructed with "needles"; Fig. 2e), the mean height of the histogram (m.h.h.) for basic lysozyme is much smaller than that for acidic BSA [*cf.*, parts (a) and (a′) and parts (e) and (e′), respectively]. With both HA type S_1 (Fig. 2b) and "rose des sables"-like HA (Fig. 2f), the m.h.h. for lysozyme is slightly smaller than that for BSA (*cf.*, Fig. 3b and b′, and Fig. 3f and f′, respectively), in contrast to HA type F (Fig. 2d) for which the m.h.h. for BSA is slightly smaller than that for lysozyme (*cf.*, Fig. 3d and d′). With HA type H (Fig. 2c), the m.h.h. for BSA is considerably smaller than that for lysozyme (*cf.*, Fig. 3c and c′).

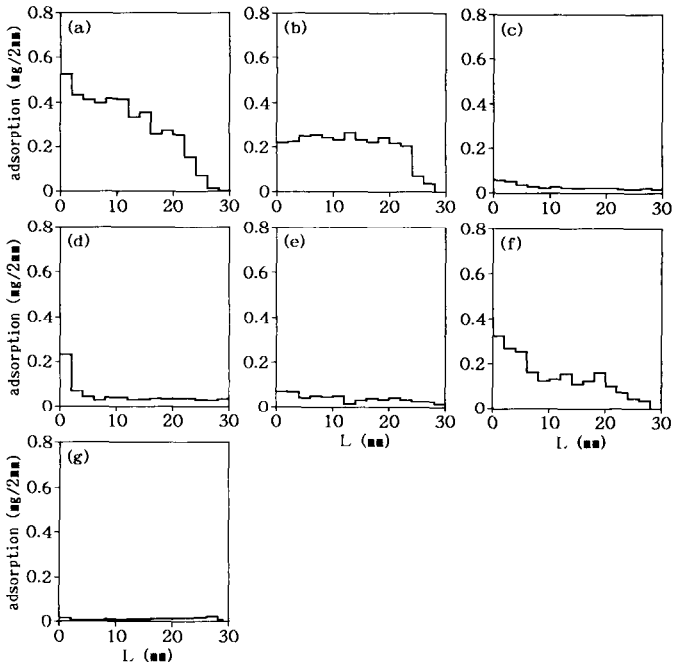

Fig. 4. As Fig. 3, obtained by using the column packed with coral HA for (a) pepsinogen, (b) ovalbumin, (c) myoglobin, (d) trypsinogen, (e) RNase A, (f) cytochrome *c* and (g) cytochrome *c*. The experiments were carried out in the presence of 1 m*M* KP (a–f) or 50 m*M* KP (g).

The histograms in Fig. 4 were obtained by using columns packed with coral HA for five other proteins: (a) pepsinogen (p*I* = 3.9); (b) ovalbumin (p*I* = 4.6); (c) myoglobin (p*I* = 7.0); (d) trypsinogen (p*I* = 9.3); (e) RNase A (p*I* = 9.7); and (f) and (g) cytochrome *c* (p*I* = 9.8–10.0); the histograms in Fig. 4a–f and Fig. 4g were obtained in the presences of 1 and 50 m*M* KP, respectively. It can be seen in Fig. 4 that the m.h.h.s for proteins with p*I* $\geqslant$ 7, except that for cytochrome *c* in the presence of 1 m*M* KP, are much smaller than the m.h.h.s for proteins with p*I* < 7.

The histograms in Fig. 5 were obtained by using columns packed with HA type S_1, and parts (a)–(g) correspond to (a)–(g) in Fig. 4, respectively. It can be seen in Fig. 5 that the m.h.h.s for all proteins are of the same order of magnitude, independent of p*I*. The m.h.h. for cytochrome *c* in the presence of 1 m*M* KP is exceptionally prominent, however (Fig. 5f). Fig. 5f can be compared with Fig. 4f, where the m.h.h. is exceptionally large among those for basic proteins.

The histograms in Fig. 6 were obtained in the presence of 1 m*M* KP by using columns packed with HA type S_1 for several types of protein mixtures. Independent histograms for the respective components of the mixture are also drawn, the amounts of the components being equal to those in the mixture. Thus, Fig. 6a and b relate to mixtures of acidic proteins, *i.e.*, a mixture of BSA and pepsinogen, and a mixture of BSA and ovalbumin, respectively. Fig. 6c is for a mixture of basic proteins, lysozyme and cytochrome *c*. Fig. 6d and e refer to mixtures of acidic and basic proteins, *i.e.*, a mixture of BSA and lysozyme and a mixture of BSA and cytochrome *c*, respectively.

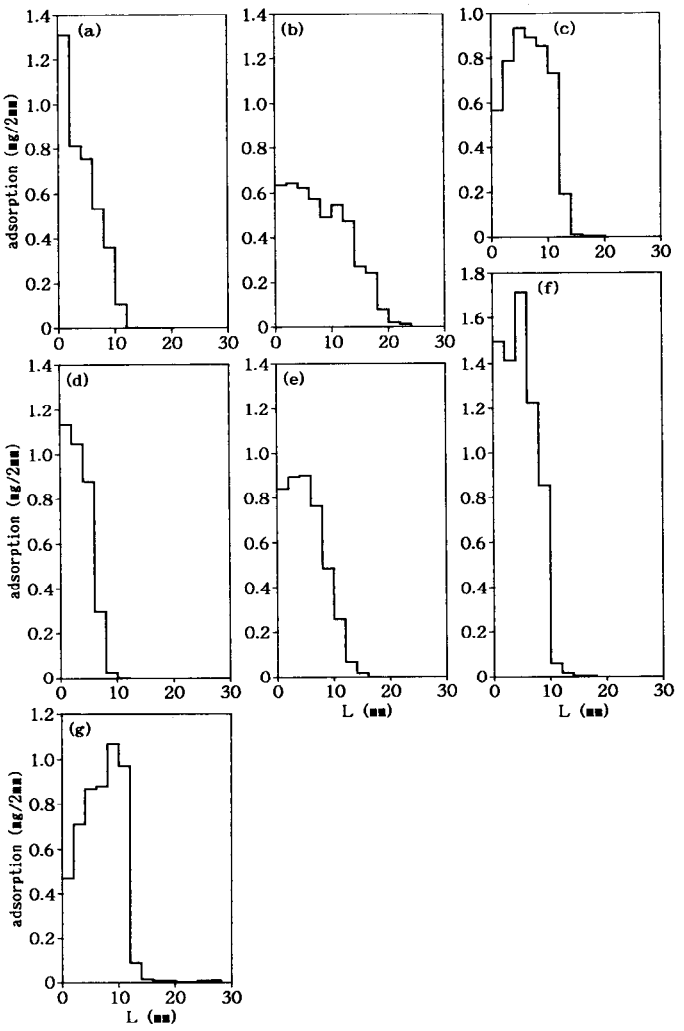

Fig. 5. As Fig. 4, obtained by using the column packed with HA type S_1.

It can be seen in Fig. 6 that, with both the mixture of acidic proteins (a and b) and the mixture of basic proteins (c), the width of the total histogram is roughly equal to the sum of the widths of the indepedent histograms for the respective components. With the mixtures of acidic and basic proteins, however, the height of the total histogram is roughly equal to the sum of the heights of the independent histograms for the respective components (see Fig. 6d and e).

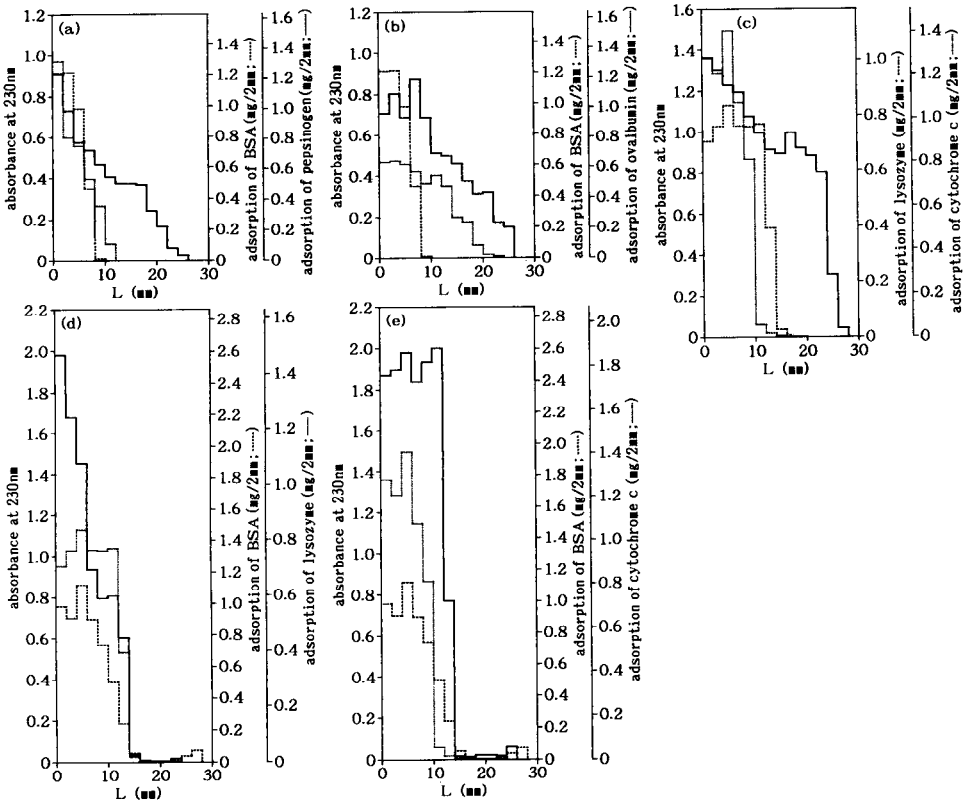

Fig. 6. As Fig. 3, obtained in the presence of 1 m*M* KP by using the column packed with HA type S_1 for mixtures of (a) BSA and pepsinogen, (b) BSA and ovalbumin, (c) lysozyme and cytochrome *c*, (d) BSA and lysozyme and (e) BSA and cytochrome *c*. (The histograms for the mixtures were drawn by using a continuous line.) Independent histograms for the respective components of the mixture are also shown, where the amounts of the components are equal to those appearing in the mixture. [The independent histograms were drawn by using two types of dotted line. Independent histograms for pepsinogen in (a), ovalbumin in (b), lysozyme in (c), BSA in (d), lysozyme in (d) and BSA in (e) are reproduced from Figs. 5a, 5b, 3b', 3b, 3b' and 3b, respectively.] On the left-hand ordinate, the absorbance at 230 nm of the supernatant (see Experimental) is indicated instead of the amount of molecules adsorbed per 2-mm slice of the column contents. These amounts for the respective components of the mixture in the independent histograms are indicated on the right-hand ordinate.

HPLC experiments and their analysis[a]

The proteins considered here are pepsinogen (p*I* = 3.9), ovalbumin (p*I* = 4.6), BSA (p*I* = 4.7), β-lactoglobulin A (p*I* = 5.1–5.3), myoglobin (p*I* = 7.0), trypsinogen (p*I* = 9.3), RNase A (p*I* = 9.7), cytochrome *c* (p*I* = 9.8–10.0), lysozyme (p*I* = 10.5–11.0) and fractions I, II and III of IgG; fractions I and II and fraction III are assemblies of "basic" and "acidic" molecules, respectively (for the three fractions of IgG, see Appendix II in Part II[2]).

[a] See Part II[2] for double gradient chromatography, the method of analysis of the experimental results and experimental parameters that are used in this sub-section.

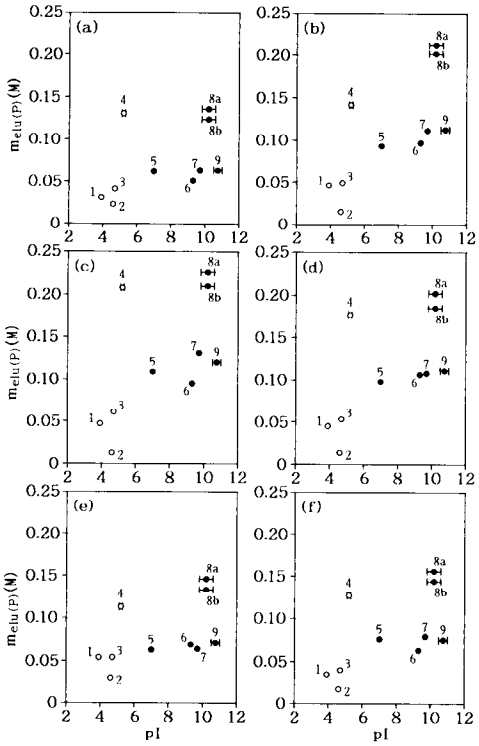

Fig. 7. Plots of $m_{elu(P)}$ *versus* p*I* for (1) pepsinogen, (2) ovalbumin, (3) BSA, (4) β-lactoglobulin A, (5) myoglobin, (6) trypsinogen, (7) RNase A, (8a) cytochrome *c* in reduced state, (8b) cytochrome *c* in oxidized state and (9) lysozyme, obtained by using columns packed with (a) coral HA, (b) HA type S_1, (c) HA type H, (d) HA type F, (e) potato-like HA and (f) "rose des sables"-like HA; ○ and ● correspond to "acidic" and "basic" molecules, respectively. In all the experiments, the total length, *L*, of the column was fixed at 13 cm, and the slope, $g'_{(P)}$ (ϕ = 1 cm) = 2.5 m*M*/ml, of the KP gradient was applied. The two points (8a and 8b) for cytochrome *c* in (a) were obtained by interpolation by using theoretical curves, however (*cf.*, Fig. 8a where the theoretical curve for cytochrome *c* in reduced state is drawn). The points (except for β-lactoglobulin A) in (b) correspond to data shown in the tenth column in Table I in Part II[2]. Other experimental conditions: (a) sample load, 30–100 μg; flow-rate, 0.50 ml/min; *P*, 1.5–4.0 MPa; *T*, 24.5–26.5°C; (b) sample load, 25–300 μg; flow-rate, 0.49–0.51 ml/min; *P*, 1.3–2.4 MPa; *T*, 23.2–29.7°C; (c) sample load, 30–400 μg; flow-rate, 0.50–1.01 ml/min; *P*, ≤0.2 MPa; *T*, 24.5–27.0°C; (d) sample load, 10–275 μg; flow-rate, 0.50–1.01 ml/min; *P*, 0.2–0.5 MPa; *T*, 24.5–27.0°C; (e) sample load, 35–90 μg; flow-rate, 0.50–0.51 ml/min; *P*, ≤0.2 MPa; *T*, 24.0–26.0°C; and (f) sample load, 28–94 μg; flow-rate, 0.50–0.51 ml/min; *P*, ≤0.2 MPa; *T*, 23.0–26.2°C.

Preliminarily, double gradient HPLC of all these proteins except IgG was carried out by using columns packed with coral HA, HA type S_1, HA type H, HA type F, potato-like HA and "rose des sables"-like HA. It was confirmed that, with any type of HA, pepsinogen, ovalbumin, BSA and β-lactoglobulin A behave as "acidic" molecules, eluted from the column with the second KP gradient in the double gradient system; myoglobin, trypsinogen, RNase A, cytochrome *c* and lysozyme behaved as "basic" molecules, eluted with the first KCl gradient in the system (*cf.*, Part II[2]). In some instances with both pepsinogen and ovalbumin, however, a minor proportion of the molecules was eluted with a rapid decrease in KCl molarity occurring at the end of

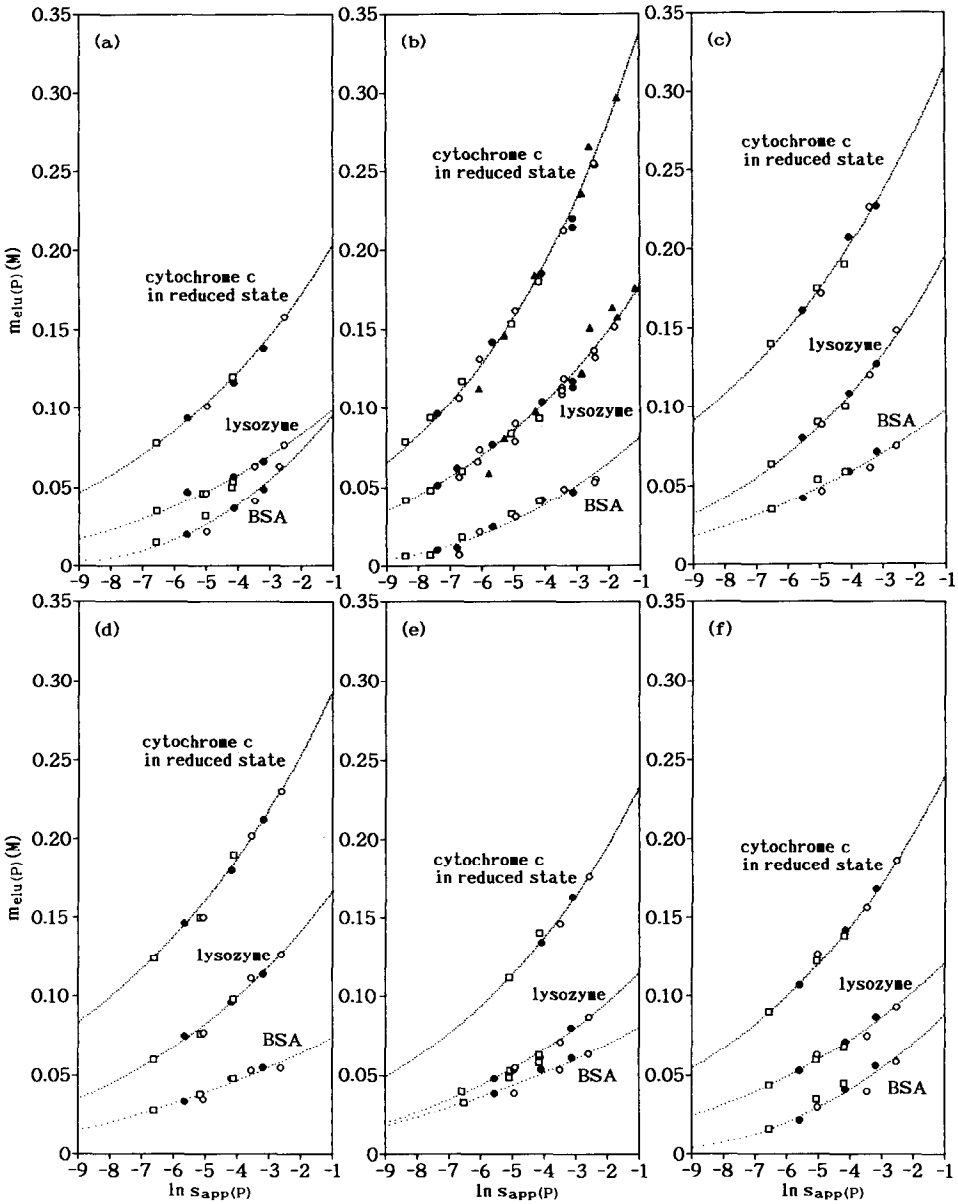

Fig. 8. Points: experimental plots of $m_{elu(P)}$ *versus* ln $s_{app(P)}$ for BSA, lysozyme and cytochrome *c* in reduced state, obtained by using columns packed with (a) coral HA, (b) HA type S_1, (c) HA type H, (d) HA type F, (e) potato-like HA and (f) "rose des sables"-like HA. The $g'_{(P)}$ (ϕ = 1 cm) values applied were (▲) 5.0, (○) 2.5, (●) 1.25 and (□) 0.45 m*M*/ml. Other experimental conditions: (a) sample load, 30–150 μg; flow-rate, 0.46–0.52 ml/min; *P*, 0.1–0.6 MPa; *T*, 21.0–29.7°C; (b) sample load, 16–480 μg; flow-rate, 0.46–0.51 ml/min; *P*, 0.3–10.0 MPa; *T*, 21.0–29.7°C; (c) sample load, 30–200 μg; flow-rate, 0.50–0.51 ml/min; *P*, ≤0.4 MPa; *T*, 23.8–25.1°C; (d) sample load, 30–150 μg; flow-rate, 0.50 ml/min; *P*, 0.2–0.6 MPa; *T*, 23.0–26.0°C; (e) sample load, 27–150 μg; flow-rate, 0.50–0.51 ml/min; *P*, ≤ 0.2 MPa; *T*, 23.3–27.0°C; and (f) sample load, 28–145 μg; flow-rate, 0.50–0.51 ml/min; *P*, ≤ 0.2 MPa; *T*, 23.5–27.0°C. Curves: theoretical curves calculated by using eqn. 6 in ref. 2; for the parameters involved in the equation, see Table I. [Both the experimental points and the theoretical curves in (b) are reproduced from ref. 2.]

TABLE I

SUMMARY OF RESULTS OF GRADIENT HPLC EXPERIMENTS CARRIED OUT USING A VALUE OF THE PARAMETER φ OF 25 M^{-1} (*CF.*, FIGS. 8–10)

The analyses for pepsinogen, ovalbumin, myoglobin, trypsinogen and RNase A were performed for the main peak of the chromatogram.

Protein	*HA*	x'	$\ln q_{app(P)}$	*Protein*	*HA*	x'	$\ln q_{app(P)}$	*Protein*	*HA*	x'	$\ln q_{app(P)}$
"Acidic" proteins:				*"Basic" proteins:*				RNase A	Coral	5.0	5.9
BSA	Coral	4.5	2.8	Lysozyme	Coral	6.5	7.4		S_1	4.3	6.9
	S_1	6.0	3.6		S_1	5.7	9.5	IgG fraction I	Coral	11.0	10.4
	H	8.2	6.9		H	5.0	8.7		S_1	11.0	11.2
	F	10.0	6.9		F	6.0	9.7		H	9.5	12.4
	Potato	10.0	7.5		Potato	6.2	7.8		F	11.0	12.7
	"Rose des sables"	5.5	3.5		"Rose des sables"	6.5	8.6		Potato	9.0	10.1
Ovalbumin	Coral	5.0	1.2	Cytochrome *c* (in reduced state)	Coral	6.0	10.9		"Rose des sables"	12.0	13.9
	S_1	8.0	0.5		S_1	4.8	11.2				
					H	6.5	14.9	IgG fraction II	Coral	11.0	15.4
IgG fraction III	Coral	17.0	23.0		F	6.5	14.4		S_1	11.0	16.6
	S_1	18.0	25.0		Potato	5.5	10.7		H	11.0	17.9
	H	15.5	22.9		"Rose des sables"	5.7	11.3		F	11.0	17.4
	F	16.0	22.7						Potato	9.0	13.3
	Potato	15.0	20.5	Cytochrome *c* (in oxidized state)	Coral	5.5	9.6		"Rose des sables"	12.0	17.9
	"Rose des sables"	19.0	26.0		S_1	4.8	10.8				
					H	5.6	12.7				
					F	6.0	12.9				
					Potato	5.5	10.2				
					"Rose des sables"	5.7	10.8				

the first KCl gradient, presumably owing to a kinetic mechanism arising from an abrupt change in the environment (*i.e.*, the KCl molarity) (for details on the kinetic mechanism, see Part I[1]). It should be stressed that the chromatographic behaviours of all proteins are similar for all the HAs that were used.

The points in Fig. 7a–f are experimental plots of $m_{elu(P)}$ *versus* p*I* for the above proteins except IgG, obtained by using columns packed with (a) coral HA, (b) HA type S_1, (c) HA type H, (d) HA type F, (e) potato-like HA and (f) "rose des sables"-like HA (the plots for pepsinogen, ovalbumin, myoglobin, trypsinogen and RNase A are concerned with the main peak of the chromatogram; all the analyses for these proteins will be performed for the main peak). In all the experiments, the total length, L, of the column was fixed at 13 cm, and the slope, $g'_{(P)}$ (ϕ = 1 cm) = 2.5 mM/ml, of the KP gradient was applied. It can be seen in Fig. 7 that, in general, "acidic" proteins tend to be eluted at lower phosphate molarities than "basic" proteins while keeping almost the same constellations of the plot among the "acidic" and the "basic" proteins, respectively. With coral HA, potato-like HA and "rose des sables"-like HA, however, the elution molarities of the "basic" proteins tend to decrease; as a result, the elution molarities of the "acidic" proteins and those of the "basic" proteins tend to approach each other (compare Fig. 7a, e and f with Fig. 7b, c and d).

The points in Fig. 8a–f are experimental plots of $m_{elu(P)}$ *versus* ln $s_{app(P)}$ for BSA, lysozyme and cytochrome *c* in reduced state, obtained by using columns packed with (a) coral HA, (b) HA type S_1, (c) HA type H, (d) HA type F, (e) potato-like HA and (f) "rose des sables"-like HA. The curves in Fig. 8 are theoretical, calculated by using eqn. 6 in Part II[2]. For the calculation, the optimum value of the parameter φ of 25 M^{-1} was used; this value will hereafter be used for all the calculations (*cf.*, ref. 2). For the other experimental parameters, the values given in Table I were applied in order to obtain best fits with the experiment. It can be seen in Fig. 8 that, with (a) coral HA, (e) potato-like HA and (f) "rose des sables"-like HA the elution molarities of "basic" proteins, lysozyme and cytochrome *c*, tend to decrease, and they approach those of "acidic" BSA; especially the elution molarities of lysozyme are close to those of BSA.

The points in Fig. 9a and b are experimental plots of $m_{elu(P)}$ *versus* ln $s_{app(P)}$ for

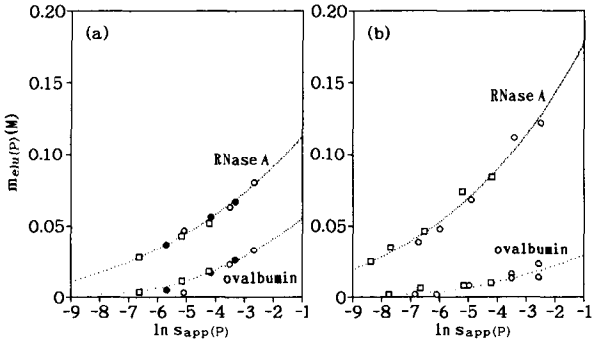

Fig. 9. Points: as Fig. 8 for ovalbumin and RNase A, obtained by using columns packed with (a) coral HA and (b) HA type S_1. The $g'_{(P)}$ (ϕ = 1 cm) values applied were (○) 2.5, (●) 1.25 and (□) 0.45 mM/ml. Other experimental conditions: (a) sample load, 35–50 μg; flow-rate, 0.50 ml/min; P, 0.1–0.5 MPa; T, 24.0–27.0°C; and (b) sample load, 25–300 μg; flow-rate, 0.50 ml/min; P, 0.5–5.0 MPa; T, 24.0–26.6°C. Curves: as Fig. 8. [Both the experimental points and the theoretical curves in (b) are reproduced from ref. 2.]

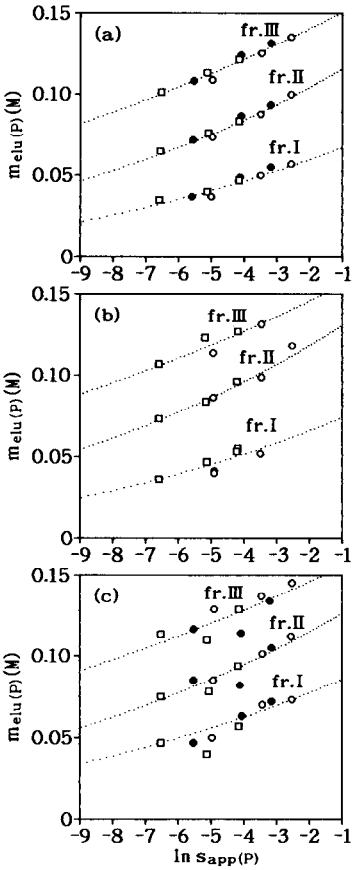

Fig. 10. Points: as Fig. 8 for fractions I, II and III of IgG, obtained by using columns packed with (a) coral HA, (b) HA type S_1 and (c) "rose des sables"-like HA. The $g'_{(P)}$ (ϕ = 1 cm) values applied were (○) 2.5, (●) 1.25 and (□) 0.45 mM/ml. Other experimental conditions: (a) sample load, 0.033–0.114 in units of absorbance (at 230 nm) × ml; flow-rate, 0.48–0.51 ml/min; P, 0.1–0.6 MPa; T, 24.5–27.7°C; (b) sample load, 0.047–0.231 in units of absorbance (at 230 nm) × ml; flow-rate, 0.49–0.50 ml/min; P, 0.9–4.9 MPa; T, 20.0–25.0°C; and (c) sample load, 0.026–0.087 in units of absorbance (at 230 nm) × ml; flow-rate, 0.50–0.51 ml/min; P, 0.1–0.2 MPa; T, 23.5–25.8°C. Curves: as Fig. 8. [Both the experimental points and the theoretical curves in (b) are reproduced from ref. 2.]

ovalbumin and RNase A, obtained by using columns packed with (a) coral HA and (b) HA type S_1; the curves are theoretical, calculated by using the parameters given in Table I. It can be seen in Fig. 9 that the elution molarities of "acidic" ovalbumin and those of "basic" RNase A approach each other more closely with coral HA (a) than with HA type S_1 (b); this tendency is parallel with that observed for other "acidic" and "basic" proteins (see Fig. 8a and b).

The points in Fig. 10a–c are experimental plots of $m_{elu(P)}$ *versus* ln $s_{app(P)}$ for "basic" fractions I and II and "acidic" fraction III of IgG, obtained by using columns packed with (a) coral HA, (b) HA type S_1 and (c) "rose des sables"-like HA; the curves are theoretical, calculated by using parameters given in Table I. It can be seen in Fig. 10

that "basic" fractions I and II are eluted at lower molarities than "acidic" fraction III, and that the relative positions among the three plots for the three fractions do not depend much on the type of HA used. Similar diagrams were also obtained by using columns packed with HA type H, HA type F and potato-like HA.

DISCUSSION

*Confirmation that, during the chromatographic process on the column, acidic proteins with pI $\lesssim$ 7 (and also nucleic acids including other nucleotides) are mainly adsorbed on the **a** (or **b**) crystal surface, that basic proteins with pI $\gtrsim$ 7 are mainly adsorbed on the **c** crystal surface and that these occur independently of the external crystal shape of HA that is used*

The above confirmation can be obtained from the following three considerations. First, in the double gradient system, acidic proteins (ovalbumin, BSA and β-lactoglobulin A) are eluted with the second KP gradient whereas basic (and neutral) proteins (myoglobin, trypsinogen, RNase A, cytochrome *c* and lysozyme) are eluted with the first KCl gradient; this occurs independently of the external crystal shape of HA used (preliminary experiment in the second sub-section of Results). The behaviour of DNA and nucleoside phosphates in the double gradient system is parallel with that of acidic proteins (see Part I[1]). Further, the constellation of the $m_{elu(P)}$ *versus* p*I* plot among the acidic proteins and the constellation of the same plot among the basic (and neutral) proteins are both almost parallel for all the HAs used, with different external shapes (Fig. 7; for slight differences in the constellation among different HAs, see the third sub-section). These data indicate that, with HA with any external shape, the crystal surface on which acidic proteins (and nucleic acids, including other nucleotides) are adsorbed is different from the surface on which basic (and neutral) proteins are adsorbed, and that the two common adsorbing surfaces appear independently of the external crystal shape of HA (*cf.*, Introduction in Part II[2]; for some related arguments, see Appendix I).

Second, with regard to coral HA constructed with hexagonal rods (Fig. 2a), only **a** and **c** surfaces appear on the crystal, and the total area of the **c** surfaces is much smaller than that of the **a** surfaces (see Introduction). On the other hand, the m.h.h.s with coral HA for basic (and neutral) proteins (lysozyme, myoglobin, trypsinogen, RNase A and cytochrome *c*) are generally much smaller than those for acidic proteins (BSA, pepsinogen and ovalbumin) (Figs. 3a and a′ and 4a–e and g) except for cytochrome *c* in the presence of 1 m*M* KP (Fig. 4f). These data indicate that, with coral HA, acidic proteins are (mainly) adsorbed on the **a** surface whereas basic (and neutral) proteins are (mainly) adsorbed on the **c** surface; the exceptional behaviour of cytochrome *c* occurring in the presence of 1 m*M* KP will be discussed in the last sub-section.

With regard to potato-like HA constructed with "needles" (Fig. 2e) also, it is highly probable that the **a** surface appears in a major proportion (see Introduction) whereas the m.h.h. for basic lysozyme is much smaller than that for acidic BSA (Fig. 3e and e′). The situation is parallel with that with coral HA (see above).

With regard to the other HAs [HA type S_1 (Fig. 2b), HA type H (Fig. 2c), HA type F (Fig. 2d) and "rose des sables"-like HA (Fig. 2f)], it is difficult to identify the crystal surface on the basis of the electron micrograph only (see Introduction).

However, it does not appear that the ratio between **a** and **c** surface areas is extremely biased except for "rose des sables"-like HA (for "rose des sables"-like HA in Fig. 2f, see the third sub-section). In fact, the ratios between m.h.h.s for acidic and basic proteins are not extremely biased with HA type S_1, HA type F and "rose des sables"-like HA (compare Fig. 3b and b′, d and d′, and f and f′, respectively; see also Fig. 5). As far as HA type H is concerned, however, the m.h.h. for acidic BSA is considerably smaller than that for basic lysozyme (Fig. 3c and c′).

All these data, together with the first part of the confirmation, indicate that acidic proteins, or more generally proteins with $pI \lesssim 7$ and nucleic acids including other nucleotides, are mainly adsorbed on the **a** surface whereas proteins with $pI \gtrsim 7$ are mainly adsorbed on the **c** surface; these occur independently of the external crystal shape of HA.

Third, the width of the total histogram for mixtures of acidic proteins (a mixture of BSA and pepsinogen and a mixture of BSA and ovalbumin) is roughly equal to the sum of the widths of the independent histograms for the respective components of the mixtures (Fig. 6a and b). The width of the total histogram for a mixture of basic proteins (lysozyme and cytochrome *c*) is also roughly equal to the sum of the widths of the independent histograms for the respective components of the mixture (Fig. 6c). These data indicate that acidic proteins are adsorbed on a common surface of HA and that basic proteins are also adsorbed on a common surface. With mixtures of acidic and basic proteins (a mixture of BSA and lysozyme and a mixture of BSA and cytochrome *c*), however, the height of the total histograms is roughly equal to the sum of the heights of the independent histograms for the respective components of the mixtures (Fig. 6d and e). These data indicate that acidic and basic proteins are adsorbed on different crystal surfaces of HA. The conclusions support those obtained in both the first and second parts of the confirmation.

Relationship with the crystal surface structure deduced from the structural study of HA

It should be recalled that the appearances of both the **a** and the **c** surfaces on the HA crystal can also be deduced from the structural study of HA with which the idea of the epitaxial crystal growth is connected (see Introduction). It should be emphasized that, from this study, the conclusion has been drawn that anion exchangers with positive charges (or adsorbing C sites) should be present on the **a** surface whereas cation exchangers with negative charges (or adsorbing P sites) should be present on the **c** surface (see Introduction). The conclusion is consistent with the considerations in the first sub-section and also those in Part I[1] (*cf.*, Introduction in Part II[2]): with HA chromatography, competition occurs between acidic proteins (or nucleic acids including other nucleotides) and phosphate ions from the buffer, and between basic proteins and cations from the buffer for adsorption on the **a** and the **c** surface of HA, respectively.

Comparison of detailed profiles of the HPLC experiments carried out by using different types of HA

In general, acidic proteins tend to be eluted at lower phosphate molarities than basic proteins (Fig. 7; see also Fig. 2 in Part II[2]). With coral HA, potato-like HA and "rose des sables"-like HA, however, the elution molarities of "basic" proteins tend to decrease and the elution molarities of "acidic" proteins and those of "basic" proteins

tend to approach each other (compare Fig. 7a, e and f with Fig. 7b, c and d, Fig. 8a, e and f with Fig, 8b, c and d, and Fig. 9a with Fig. 9b), except for IgG, the elution profile of which does not depend much on the type of HA used (Fig. 10). The elution profiles of the proteins, including the exceptional behaviour of IgG, can be explained qualitatively by the fact that, with both coral HA and potato-like HA, the total area of the **c** surfaces on which the adsorption of "basic" proteins occurs is much smaller than the total area of the **a** surfaces on which the adsorption of "acidic" proteins occurs (see Appendix II; for "rose des sables"-like HA, see below).

Monma *et al.*[13] performed an electron diffraction analysis of an HA crystal with an external shape very similar to that of "rose des sables"-like HA, the surface of which is covered by lamellae (Fig. 2f). They reported that the flat surface of a lamella corresponds to the (100) or the **a** surface as deduced from the electron diffraction pattern. It is therefore highly probable that the flat surface of a lamella of "rose des sables"-like HA also corresponds to the **a** surface, and that the major proportion of the total surface of the lamella is occupied by the **a** surface. This deduction appears to be compatible with the fact that, with "rose des sables"-like HA also, the elution molarities of "basic" proteins tend to decrease (Figs. 7f and 8f) in parallel with both cases for coral HA and potato-like HA (Figs. 7a and e, and 8a and e). As far as the adsorption experiment is concerned, however, the m.h.h. for "acidic" BSA is only slightly larger than that for "basic" lysozyme with "rose des sables"-like HA (Fig. 3f and f'); this can be compared with both cases for coral HA and potato-like HA in which the m.h.h. for "acidic" BSA is much larger than that for "basic" lysozyme (Fig. 3a, a', e and e'). This experimental result implies that, on the total surface of "rose des sables"-like HA, non-lamellar structures are also involved in part. Consistent with this deduction, non-lamellar structures can be found on the crystal surface of "rose des sables"-like HA by careful examination of the electron micrograph (not shown). In order to continue the argument, further experimental data are needed.

Table I summarizes both x' and $\ln q_{app(P)}$ values calculated on the basis of Figs. 8–10 for several proteins with different types of HA; for IgG with HA type H, HA type F and potato-like HA, additional data were used for the calculations. All the calculations were performed in order for the theoretical curve (represented by eqn. 6 in Part II[2]) to coincide best with the experimental plot by using the optimum value of the parameter φ of 25 M^{-1} (for the value of φ, see ref. 2). It can be seen in Table I that, except for BSA and ovalbumin, the x' value, representing the number of adsorbing sites (C or P) on the HA surface covered by an adsorbed sample molecule[2], is nearly constant, independent of the type of HA used. The considerable fluctuations in the x' value that occur with both BSA and ovalbumin are artifacts, arising from the difficulty in carrying out precise evaluations of the parameter when the molecule is eluted with low phosphate molarities (see Figs. 8 and 9).

The constellation of the $m_{elu(P)}$ *versus* p*I* plot among the "acidic" proteins and the constellation of the same plot among the "basic" proteins, both representing only weak correlations (if they exist) between $m_{elu(P)}$ and p*I*, are almost parallel among different types of HA (Fig. 7; *cf.*, first sub-section). This, together with the fact that x' is nearly constant, independent of the type of HA (except for the fluctuations arising from the artifact; see above), leads to the deduction that the surface of a domain on the HA crystal on which the molecular adsorption takes place is fairly smooth, and that the size of the domain under consideration is larger than the size of the proteins that

have been applied. The size of the smooth domain is larger than 100–200 Å, the size of IgG (the largest molecule that has been applied; see Fig. 13 in Part II[2]). This means that the size of the crystallites that constitute the total crystal is larger than 100–200 Å. It should be recalled that the chromatographic properties of several types of HA prepared by using different methods were studied by Spencer[14] in connection with both the crystal surface structure (as observed by scanning electron microscopy) and the size of the crystallites constituting the total HA particle (as deduced from the X-ray diffraction profile). On the basis of some reasonable assumption, he deduced that the elution phosphate molarity of tRNA (with the longest dimension of about 90 Å for one of the smaller species) increases with increase in the smallest dimension of the crystallite faces if it is less than 110 Å; if it exceeds 110 Å, the elution molarity of tRNA is virtually constant, independent of the crystallite size[14]. This suggests that, for optimum binding, the smallest dimension of the crystallite faces needs to exceed the size of the molecule[14].

It can be seen in Table I that the x' values of 15.0–19.0 for "acidic" IgG are larger than the corresponding values of 9.0–12.0 for "basic" IgG's. As pointed out in Part II[2], this is compatible with the deduction that two C sites are present per unit cell on the **a** surface of HA whereas only a single P site is present per unit cell on the **c** surface (see Introduction); the size of the smooth domain on the HA surface where the molecular adsorption takes place is larger than the size of an IgG molecule (see above). [It should be recalled that the x' values were calculated by using the optimum value of the parameter φ of 25 M^{-1}. If the lower or the upper limit value of φ is assumed, the x' values deviate considerably from the values that are given in Table I (see Table I in Part II[2] and also Figs. 11 and 12 in Part II[2]). The ratios among the x' values for different proteins are kept virtually constant if the φ value varies, however.]

The constellation of the $m_{elu(P)}$ *versus* p*I* plot is slightly different among the different HAs that were used (Fig. 7). This, together with the slight fluctuation in the x' value (in addition to that arising from the artifact; see Table I), might reflect certain minor defects in the crystal surface structure which might occur in different manners on the smooth domains of the surfaces of different types of HA. It does not appear, however, that the non-stoichiometric Ca/P molar ratio in some HAs (see Introduction) is effectively related to the defect in the crystal surface structure under consideration; this is because no direct correlation has so far been found between the chromatographic properties of HA and the Ca/P molar ratio. [At the 8th Conference on Liquid Chromatography, Tokyo (1987), the influence of the Ca/P molar ratio on the elution molarity of proteins was reported orally by Inoue *et al.* No proof was given, however, concerning whether or not the elution molarity is *directly* influenced by the Ca/P molar ratio of HA. The possibility cannot be excluded that a slight change in the Ca/P molar ratio occurring on the crystal surface of HA affects the network structure of water molecules that keep in contact with the HA crystal, and that this brings about a slight change in the elution molarity of proteins. Also, no detailed investigation on the surface structure of HAs that were used in this study was performed.] In Part I[1], it was pointed out that the **a** surface of some commercially available spherical HA particles is damaged to a considerable extent.

Exceptional adsorption of cytochrome c in the presence of 1 mM KP

With coral HA, the m.h.h.s for basic (and neutral) proteins occurring in the

presence of 1 m*M* KP are generally much smaller than those for acidic proteins occurring in the presence of 1 m*M* KP (Figs. 3a and a′, and 4a–e); the m.h.h. for basic cytochrome *c* in the presence of 1 m*M* KP is exceptionally large (Fig. 4f). The m.h.h. for cytochrome *c* in the presence of 50 m*M* KP is as small as those for the other basic proteins occurring in the presence of 1 m*M* KP, however (Fig. 4g). With HA type S_1, the m.h.h.s for all the proteins in the presence of 1 m*M* KP (Figs. 3b and b′, and 5a–f) and the m.h.h. for cytochrome *c* in the presence of 50 m*M* KP (Fig. 5g) are of the same order of magnitude. The m.h.h. for cytochrome *c* in the presence of 1 m*M* KP is exceptionally prominent, however (Fig. 5f).

It can be considered that the exceptionally large m.h.h.s for cytochrome *c* in the presence of 1 m*M* KP (Figs. 4f and 5f) are connected with the fact that the molarity of the KP buffer used, 1 m*M*, is exceptionally *much* lower than the molarity at which the transition of the *B′* value from *ca.* 0 to 1 begins (see Fig. 5d and e in Part II[2]). In fact, with regard to the other proteins that were examined (BSA, lysozyme, pepsinogen, ovalbumin, myoglobin, trypsinogen and RNase A), 1 m*M* is close to the molarity at which the transition of the *B′* value begins (*cf.*, Fig. 4d and e, and Fig. 7c and d in Part II[2] for HA type S_1; the statement was also confirmed for the other types of HA). A molarity of 50 m*M* with cytochrome *c* is also close to that at which the transition of the *B′* value begins (*cf.*, Fig. 5d and e in Part II[2] for HA type S_1; the statement was also confirmed for the other types of HA).

In an earlier paper[15], it was pointed out that, when the development of the molecules is in progress under overload conditions, repulsive forces reside among sample molecules that remain on the adsorbent surfaces in the column. This means that the surface of any molecule in the stationary state keeps in contact with the adsorbent surface at least partially when the development of the molecules is in progress in the column. In other words, the formation of multi-layers of molecules on the adsorbent surface is impossible at least when the development of the molecules is in progress in the column; this is because it is repulsive forces, and not attractive forces, that reside among molecules in the stationary state (see above). It was demonstrated previously[16] that the chromatographic behaviour of chicken and turkey lysozymes and a mixture of them under overload conditions can be explained quantitatively by assuming the participation of repulsive molecular interactions.

The development of molecules on the HA column is possible only when *B′* is larger than *ca.* 0 (*cf.*, the "first principle of chromatography in general" mentioned in Appendix III in ref. 17) or when the molarity of the KP buffer is higher than the molarity at which the transition of the *B′* value from *ca.* 0 to 1 begins. This means that the m.h.h.s for BSA, lysozyme, pepsinogen, ovalbumin, trypsinogen and RNase A occurring in the presence of 1 m*M* KP and also the m.h.h. for cytochrome *c* occurring in the presence of 50 m*M* KP are all close to those that should be realized when the maximum possible number of molecules is adsorbed on the HA surface, fulfilling the condition that the surface of any molecule keeps in contact with the crystal surface of HA at least partially.

It can be deduced that the large m.h.h. for cytochrome *c* occurring in the presence of 1 m*M* KP (Figs. 4f and 5f) arises from the formation of multi-layers on the crystal surface of HA due to weak attractive interactions among molecules. With an increase in KP molarity from 1 to 50 m*M*, the multi-layers would be released as the molecules in the layers are fixed only weakly to one another. It can also be deduced that

a single layer finally survives in which all the molecules keep in contact with the crystal surface owing to strong attractive forces towards the crystal surface of HA; repulsive forces reside among the molecules that keep in contact with the crystal surface (see above).

APPENDIX I

To the argument for the first step of the confirmation in the first sub-section under Discussion, it should be added that the chromatographic behaviour of proteins as a function of p*I* changes continuously at about p*I* $\approx$ 7, although it occurs very abruptly (see first sub-section of Discussion and the Introduction in Part II[2]). In fact, it was pointed out in Part I[1] that the elution molarity, $m_{elu(KCl)}$, of myoglobin (with a neutral p*I* of 7) in the KCl gradient system is 2.3 times higher than the potassium elution molarity, $m_{elu(K^+;KP)}$, in the KP gradient system under certain experimental conditions. This means that, although myoglobin behaves as a "basic" molecule in the double gradient system, mainly adsorbed to one of the two surfaces of HA where basic molecules should be adsorbed (*i.e.*, the **c** surface), it is partially adsorbed on the other surface where acidic molecules should be adsorbed (*i.e.*, the **a** surface); the Boltzmann distribution between the two manners of adsorption is not extremely biased towards one of them with this neutral protein (see Introduction in Part II[2]). Slight increases in $m_{elu(KCl)}$ in comparison with $m_{elu(K^+;KP)}$ were also observed for cytochrome *c*, haemoglobin, trypsinogen and RNase A (for details, see Part I[1]). This indicates that, even with basic proteins, a minor proportion of molecules are adsorbed on the crystal surface where acidic molecules should be adsorbed (*i.e.*, the **a** surface). Parallel tendencies were reconfirmed in the preliminary experiment in the second sub-section of Results and also for fractions I and II of IgG in the double gradient experiment reported in Appendix II in Part II[2].

It should also be added that the chromatographic behaviour of proteins as a function of p*I* in the $CaCl_2$ system is fundamentally almost parallel to the behaviour in the KCl system (*cf.*, Introduction in Part II[2]). Both myoglobin and trypsinogen, which behave as "basic" molecules in the KCl system, behave as "acidic" molecules in the $CaCl_2$ system, however[1]. Further, the adsorption of "acidic" proteins on the HA surface is generally stabilized in the presence of calcium ions in the mobile phase[1]. It can be suggested that, when a carboxyl group of the molecule has been adsorbed on a C site constructed with two crystal calcium ions (see Introduction), a calcium ion from the mobile phase is also fixed on the C site, completing a triangular array of calcium ions around the carboxyl group (*cf.*, Fig. 1b). The structure constructed with three calcium ions and a carboxyl group would resemble the corresponding structure in the interior of the crystal occurring when one (or two) hydroxyl ion(s) is (are) replaced by a carbonic ion (*cf.*, Introduction). On the basis of this mechanism, the adsorption of a carboxyl group on a C site would be stabilized in the presence of calcium ions in the mobile phase. It can also be suggested that the behaviour of both myoglobin and trypsinogen as "acidic" molecules in the presence of calcium ions in the mobile phase (see above) is intimately related to this adsorption mechanism.

APPENDIX II

The elution molarity, $m_{elu(P)}$ or μ, in gradient chromatography can be represented by eqn. 6 in Part II[2]. The parameter q in this equation [intimately related to the parameter $q_{app(P)}$ in Table I; *cf.*, eqns. 15 and 15′ in ref. 2], is defined by both eqns. 27 and 28 in ref. 18 as

$$q = An_0/V \tag{1}$$

where A is a positive constant, n_0 the total number of adsorbing sites (C or P) on the HA surfaces involved in an elementary volume of the column, and V the total volume of the interstitial part of the elementary volume [in ref. 18, q is written as $q_{(\rho')}$, however].

It can now be understood that, with both the coral HA packed column and the potato-like HA packed column, the n_0/V value with respect to P sites existing on the **c** surface of HA is much smaller than the corresponding value with respect to C sites existing on the **a** surface. On the basis of eqn. 6 in ref. 2, it can be shown that, in general, the elution molarity, $m_{elu(P)}$, decreases with decrease in the n_0/V value. It can also be shown that, provided that the $m_{elu(P)}$ value is kept within the same order of magnitude, the dependence of $m_{elu(P)}$ on n_0/V decreases with increase in x', which is also involved in eqn. 6 in ref. 2; when $x' = \infty$, then $m_{elu(P)}$ is independent of n_0/V. The decrease in the dependence of $m_{elu(P)}$ on n_0/V with increase in x' is intimately related to the fact that the transition of the B' value (*cf.*, eqn. 5 in ref. 2) from *ca.* 0 to 1 that occurs with an increase in the phosphate or potassium molarity, $m_{(P)}$ or $m_{(K^+)}$, becomes sharp with an increase in x', provided that the transition occurs within a molarity range of the same order of magnitude (*cf.*, Figs. 4–9 in ref. 2).

It can be seen in Table I that the x' values of 15.0–19.0 for "acidic" IgG are considerably larger than the corresponding values of 4.5–10.0 for the other "acidic" proteins, and that the x' values of 9.0–12.0 for "basic" IgGs are also considerably larger than the corresponding values of 4.3–6.5, for the other "basic" proteins. The theory gives a qualitative explanation for why the elution molarities of "basic" proteins other than IgG tend to decrease with both coral HA and potato-like HA (and also, perhaps, with "rose des sables"-like HA), and why the elution molarities of "acidic" proteins other than IgG and those of "basic" proteins other than IgG tend to approach each other with these HAs. The theory also explains why the elution profile of IgG with large x' values does not depend much on the type of HA used.

ACKNOWLEDGEMENTS

The authors are grateful to Dr. H. Monma, National Institute for Research in Inorganic Materials, for kindly taking the scanning electron micrographs of hydroxyapatite. They also thank Mr. W. Kobayashi for carrying out some experiments.

REFERENCES

1 T. Kawasaki, *J. Chromatogr.*, submitted for publication.
2 T. Kawasaki, M. Niikura and Y. Kobayashi, *J. Chromatogr.*, 515 (1990) 91.
3 M. I. Kay, R. A. Young and A. S. Posner, *Nature (London)*, 204 (1964) 1050.

4 K. Sudarsanan and R. A. Young, *Acta Crystallogr., Sect. B*, 25 (1969) 1534.
5 J. C. Elliott, P. E. Mackie and R. A. Young, *Science*, 180 (1973) 1055.
6 R. A. Young, *Colloq. Int. CNRS*, No. 230 (1973) 21.
7 T. Kawasaki, *J. Chromatogr.*, 151 (1978) 95.
8 T. Kawasaki, *J. Chromatogr.*, 157 (1978) 7.
9 W. E. Brown, *Nature (London)*, 196 (1962) 1048.
10 D. R. Taves and R. C. Reedy, *Calcif. Tissue Res.*, 3 (1969) 284.
11 S. M. Krane and M. J. Glimcher, *J. Biol. Chem.*, 237 (1962) 2991.
12 K. Lonsdale, *Nature (London)*, 217 (1968) 56.
13 H. Monma, S. Ueno, M. Tsutsumi and T. Kanazawa, *Yogyo-Kagaku-Shi*, 86 (1978) 28.
14 M. Spencer, *J. Chromatogr.*, 166 (1978) 423.
15 T. Kawasaki, *Sep. Sci. Technol.*, 24 (1989) 1109.
16 T. Kawasaki and M. Niikura, *Sep. Sci. Technol.*, 25 (1990) in press.
17 T. Kawasaki, *Sep. Sci. Technol.*, 22 (1987) 121.
18 T. Kawasaki, *Sep. Sci. Technol.*, 23 (1988) 1105.